Atmos. Chem. Phys. Discuss., doi:10.5194/acp-2016-228, 2016
Manuscript under review for journal Atmos. Chem. Phys.
Published: 17 March 2016

Atmospheric Chemistry and Physics Discussions

Ambient measurement of fluorescent aerosol particles with a WIBS in the Yangtze River Delta of China: potential impacts of combustion-generated aerosol particles

X. Yu[1,2], Z. Wang[2], M. Zhang[2], U. Kuhn[2], Z. Xie[1], Y. Cheng[2], U. Pöschl[2], H. Su[2]

[1]School of Earth and Space Sciences, University of Science and Technology of China, Hefei 230026, China

[2]Multiphase Chemistry Department, Max Planck Institute for Chemistry, Mainz 55128, Germany

Correspondence to Zhibin Wang (zhibin.wang@mpic.de) and Zhouqing Xie (zqxie@ustc.edu.cn)

Atmos. Chem. Phys. Discuss., doi:10.5194/acp-2016-228, 2016
Manuscript under review for journal Atmos. Chem. Phys.
Published: 17 March 2016

Atmospheric Chemistry and Physics Discussions

Abstract

Fluorescence characteristics of aerosol particles in polluted atmosphere were studied using a wideband integrated bioaerosol spectrometer (WIBS-4A) in Nanjing, Yangtze River Delta area of China. We observed strong diurnal and day-to-day variations of fluorescent aerosol particles (FAPs). The ratios of FAPs to total aerosol particles (1-15 μm) increased with increasing particle size and finally reached ~100%. The average number concentrations of FAPs (1-15 μm) detected in the three WIBS measurement channels (FL1: 0.6 cm^{-3}, FL2: 3.4 cm^{-3}, FL3: 2.1 cm^{-3}) were much higher than those observed in forests and rural areas, suggesting that FAPs other than bioaerosols were detected. We found that the number fractions of FAPs were positively correlated with the black carbon mass fraction, especially for the FL1 channel, indicating a large contribution of combustion-generated aerosols. To distinguish bioaerosols from combustion-generated FAPs, we investigated two classification schemes for use with WIBS data. Our analysis suggests a strong size dependence for the fractional contributions of different types of FAPs. In the FL3 channel, combustion-generated particles seem to dominate the 1-2 μm size range while bioaerosols dominate 2-5 μm. The number fractions of combustion-generated particles and non-combustion-generated particles were ~11% and ~5%, respectively.

Atmos. Chem. Phys. Discuss., doi:10.5194/acp-2016-228, 2016
Manuscript under review for journal Atmos. Chem. Phys.
Published: 17 March 2016

Atmospheric Chemistry and Physics Discussions

1 Introduction

From the beginning of atmospheric aerosols studies, airborne biological particles have been found as an important class of aerosol particles (Bary et al., 1887; Haldane and Anderson, 1887; Després et al., 2012). They are ubiquitous in the atmosphere with a wide size range from approximately several nanometers to a few hundred micrometers (Pöschl, 2005; Després et al., 2012). Primary biological aerosol particles (PBAPs) are a subset of biological particles, usually defined as the aerosols of biological origin or carry living organisms, including viruses, bacteria, fungal, pollen, cell or plant debris and animal tissue (Huffman et al., 2012). PBAPs can affect the Earth's radiation balance directly by absorbing and scattering solar radiation, and indirectly by serving as giant cloud condensation nuclei (CCN) and ice nuclei (IN), and thereby influence cloud microphysical and climate-relevant properties (Christner et al., 2008; Pöschl et al., 2010; DeLeon-Rodriguez et al., 2013; Morris et al., 2013). These impacts are not only restricted to a local scale, but may also be effective in a regional scale due to the transport of bioaerosols, e.g., by dust storms (Griffin, 2007; Polymenakou et al., 2008; Hallar et al., 2011; Creamean et al., 2013). In addition, PBAPs can spread human, animal and plant disease and influence public health (Després et al., 2012; Cao et al., 2014). Considering its comprehensive impacts in diverse scientific fields, a better understanding of PBAPs such as its concentration, composition, spatial and temporal variability becomes critically important.

Despite its importance, information of PBAPs in the atmosphere is still very limited. Further investigation is hindered due to the lack of automatic measurement techniques. Most previous studies are based on the analysis of cultivable PBAPs or DNAs from filter samples (Henningson and Ahlberg, 1994; Duchaine et al., 2001; Yu et al., 2013). These methods are time-consuming and their results may differ depending on the cultivation condition and procedures. The low time resolution of cultivation methods makes it difficult to investigate the emission mechanisms of PBAPs, which happen at a time scale of less than a few hours.

Since most biological materials contain fluorophores, instruments based on the fluorescence detection, such as UV-APS (Ultraviolet Aerodynamic Particle Sizer) and

Atmos. Chem. Phys. Discuss., doi:10.5194/acp-2016-228, 2016
Manuscript under review for journal Atmos. Chem. Phys.
Published: 17 March 2016

Atmospheric Chemistry and Physics Discussions

WIBS (Wideband Integrated Bioaerosol Spectrometer), have recently been developed for automatic online measurements of PBAPs. UV-APS is based on the UV light-induced fluorescence (UV-LIF) method and is the first commercially available instrument for real time analysis of biological aerosols (Hairston et al., 1997; Brosseau et al., 2000). It can measure size distribution of single fluorescent aerosol particles with much higher time resolution (~5 min) and aerodynamic size resolution (from 0.54 μm to 20 μm) than traditional methods. An ultraviolet laser (355 nm) is used to excite individual aerosol particles and the fluorescence emission in the wavelength range of 420-575 nm is collected by a fluorescent detector. Compared to the UV-APS with a single excitation wavelength and emission waveband, WIBS uses two excitation (280 nm and 370 nm) and emission wavebands (310-400 nm and 420-650 nm) aiming at detecting biological fluorophores tryptophan and NAD(P)H (Nicotinamide adenine dinucleotide; Healy et al., 2012).

UV-APS and WIBS have been applied in various atmospheric environments, including rainforest (Gabey et al., 2010; Huffman et al., 2012), forest (Huffman et al., 2013; Schumacher et al., 2013; Crawford et al., 2014), rural (Healy et al., 2014), suburban (Huffman et al., 2010; Toprak and Schnaiter, 2013) and urban environments (Gabey et al., 2011; Miyakawa et al., 2015; Wei et al., 2016). Besides settled sampling sites, WIBS has also been used for airborne observations (Perring et al., 2015). In clean environments, these techniques can effectively distinguish PBAPs from other kinds of aerosol particles. For example, Huffman et al. (2012) found similar size distributions of PBAPs measured by UV-APS and scanning electron microscopy (SEM) in the Amazon rainforest.

PBAPs, however, are not the only fluorescent aerosol particles (FAPs) in the atmosphere. Other materials such as polycyclic aromatic hydrocarbon (PAH) and humic-like substances (HULIS) may also fluoresce and contribute to the measured fluorescence signals (Pöhlker et al., 2012; Healy et al., 2014; Miyakawa et al., 2015). Hence, the fluorescent information given by WIBS or UV-APS may include both fluorescent biological and non-biological particles.

In order to have a deeper insight into the ambient FAPs in polluted area, we have performed WIBS measurements in Nanjing, China in the autumn of 2013. In this study,

Atmos. Chem. Phys. Discuss., doi:10.5194/acp-2016-228, 2016
Manuscript under review for journal Atmos. Chem. Phys.
Published: 17 March 2016

Atmospheric Chemistry and Physics Discussions

we first present the number concentration of FAPs in Nanjing in comparison to previous studies. Then we demonstrate the potential impacts of combustion-generated aerosol particles in discrimination of bioaerosols under the polluted atmosphere. Finally, we introduce alternative methods to quantify the relative contributions of different fluorescent materials (combustion- and bioaerosol-type particles) to FAPs.

2 Methods and instrumentation

2.1 Site description

WIBS measurements were performed at the Station for Observing Regional Processes of the Earth System (SORPES station), Xianlin campus of Nanjing University (32.12 °N, 118.95 °E). Nanjing lies in the Yangtze River Delta with a total population of 8.18 million (data of 2013), and it's a large commercial center in the East China region. The measurement site is ~20 km in the east of the urban center. The SORPES station is located on a hill about 40 m above the surroundings. Details of this station were described by Ding et al. (2013) and Herrmann et al. (2014). A 0.75 inch stainless-steel tube inlet was installed ~3 m above the roof, and sample air was dried by a silica gel drier prior to entering the WIBS. Data were collected from 29 October to 15 November 2013.

2.2 Instruments

Measurements of FAPs were performed with a WIBS-4A. It uses the single-particle elastic scattering intensity at 535 nm to calculate the optical size of particles. The scattering signal is used to trigger the flash of two xenon lamps with UV wavelength of 280 nm and 370 nm, respectively. The fluorescent signals are recorded at two wavelength bands (310-400 nm and 420-650 nm). This results in three wavelength channels: FL1 with excitation at 280 nm and detection 310–400 nm, FL2 with excitation wavelength at 280 nm and detection wavelength at 420–650 nm, and FL3 with excitation wavelength at 370 nm and detection wavelength at 420-650 nm. Respective abbreviations are listed in Table 1. During the measurement period, we used 1 μm and ~2 μm fluorescent and non-fluorescent PSL microspheres (Duke Scientific, Inc.) for calibration. The fluorescence noise threshold is defined as:

$$E_{\mathrm{Threshold}} = E + 3\sigma \quad (1)$$

Atmos. Chem. Phys. Discuss., doi:10.5194/acp-2016-228, 2016
Manuscript under review for journal Atmos. Chem. Phys.
Published: 17 March 2016

Atmospheric Chemistry and Physics Discussions

Where E is the modal baseline and σ is the standard deviations in each channel. Particles with fluorescence signals above the noise threshold are classified as FAPs. Single-particle data were converted into a size distribution with a 5-min integration time and particles with diameter of 1-15 μm were analyzed in this study.

Meteorological data were collected with an Automatic Weather Station (CAMPBEL co., AG1000). The differential mobility particle sizer (DMPS, built at Helsinki University) was used to measure the number size distribution of sub-micron particles between 6 and 800 nm mobility diameter (Herrmann et al., 2014). Particle mass concentration below 800 nm (PM_{800}) was calculated from the measured size distributions assuming a density of 1.6 g cm^{-3} (Wang et al., 2014). A 7-wavelength "Spectrum" Aethalometer (AE-31, Magee Scientific co.) was used to measure the black carbon (BC) mass concentration $M_{BC.}$

3 Results and discussion

3.1 General characteristics of fluorescent aerosol particles

Figure 1 shows the time series of number concentrations and size distributions of total aerosol particles and FAPs during the measurement period. Total particle number concentrations varied from 2 to 49 cm^{-3}, with a mean value of 13 cm^{-3} (Table 2). The FAPs exhibited strong diurnal and day-to-day variability, as shown in Fig. 2. Number concentrations of total particles and FAPs all peaked in the morning (~08:00 local time) and reached a minimum in the afternoon (~14:00). Their similar diurnal patterns indicate the dominant effect of boundary layer development in controlling the variability of aerosol particles. To better understand the source of FAPs, we also investigated the number fraction of FAPs in total particles. The boundary layer development exerts similar effect on all kinds of aerosol particles. Thus for particles of the same origin, their ratios will remain constant and a difference in their ratios reflects their different sources. As shown in Fig. 2, the fractions of FAPs presented quite different diurnal patterns. The fractions of FL1 particles (F_{FL1}) revealed substantial diurnal differences with a clear morning peak and an early afternoon minimum. On the contrary, F_{FL3} showed a much weaker variability, implying a similar source of FAPs as the total aerosol particles.

Atmos. Chem. Phys. Discuss., doi:10.5194/acp-2016-228, 2016
Manuscript under review for journal Atmos. Chem. Phys.
Published: 17 March 2016

Atmospheric Chemistry and Physics Discussions

151 The number concentration of FAPs was dominated by FL2 fluorescent particles with
152 a mean number concentration N_{FL2} of 3.4 cm^{-3}, followed by N_{FL3} of 2.1 cm^{-3} and N_{FL1} of
153 0.6 cm^{-3} (Table 2). These number concentrations were 1~2 order of magnitudes higher
154 than those observed in clean areas where bioaerosols dominate the FAPs (Table 3). For
155 example, FAPs of 0.093 cm^{-3}, 0.15 cm^{-3} and 0.023 cm^{-3} were reported for the Amazon,
156 Borneo and Hyytiälä forests, respectively (Gabey et al., 2010; Huffman et al., 2012;
157 Toprak and Schnaiter, 2013). Since polluted areas are characterized by less plants and
158 natural biological processes, less bioaerosols are expected compared to the forests. The
159 much higher number concentration of FAPs observed in Nanjing suggests other kinds of
160 FAPs being detected by WIBS.

161 Number size distributions of FAPs are shown in Fig.1 and Fig.3. The FAPs number
162 concentration peaked at ~1 μm with a second peak at 4-5 μm and 3-4 μm for FL1 and
163 FL2, respectively. No second peak was found in FL3. Figure 3 also shows the ratio of the
164 number concentration of FAPs (N_{FLi}) to total particles (N_T) in each size. Number fractions
165 of FAPs generally increased as the particle size increased, reaching ~ 100% at 14-15 μm
166 for FL1 and FL3 channels, and at 3-4 μm for FL2 channel. These results reveal that most
167 coarse mode particles contain certain kinds of fluorophores.

168 3.2 Non-biological fluorescent aerosol particles

169 As aforementioned, not only bioaerosols but also non-biological aerosols can
170 contribute to the FAPs in Nanjing. Previous studies (Pöhlker et al., 2012; Miyakawa et al.,
171 2015; Perring et al., 2015) reported that non-biological compounds like PAH, mineral
172 dust and HULIS can also fluoresce. Several non-biological fluorophores such as SOAs,
173 pyrene, humic acid and naphthalene have fluorescent property in the same excitation and
174 emission wavelength bands of FL1 channel (Chang and Thompson, 2010; Pöhlker et al.,
175 2012). These materials originate from sources different from bioaerosols. For example,
176 PAH enriches on the surface of soot particles from biomass burning and fuel combustion,
177 challenging the interpretation of ambient particle fluorescence measurements.

178 Our sampling site is located in the vicinity of the polluted Nanjing city and is
179 intensively affected by human activities. To check the potential influences of PAH and
180 combustion processes, we compared the variability of FAPs with that of BC, on which
181 the PAHs are often coated. To minimize the impacts of transport and boundary layer

Atmos. Chem. Phys. Discuss., doi:10.5194/acp-2016-228, 2016
Manuscript under review for journal Atmos. Chem. Phys.
Published: 17 March 2016

Atmospheric Chemistry and Physics Discussions

dynamics, we compared the ratio of BC and FAPs to the total particles (roughly) in their respective size range, i.e., M_{BC}/PM_{800} and F_{FLi} instead of using absolute concentrations. Miyakawa et al. (2015) had used similar methods (using concentration instead of ratio) to identify "combustion-type" and "dust-type" aerosols in urban area. We found that M_{BC}/PM_{800} showed a good correlation with the number fraction of FAPs, especially in the FL1 channel (r=0.748, Fig.4). For FL2 and FL3 channels, the number fractions also nicely followed the variation of M_{BC}/PM_{800} except for November 8, which deteriorated the overall correlation. Since BC and PAHs are products of incomplete combustion, the similar variability suggests a large contribution from combustion-generated aerosols to the measured FAPs, especially in the FL1 channel. Our results strongly support previous results (Toprak and Schnaiter, 2013; Miyakawa et al., 2015) that FAPs (FL1 channel) may came from combustion process and anthropogenic interference.

Meanwhile, we found that particles within the same FL_i group may come from different sources. Figure 4d shows that the fractional contribution of the 3-4 μm peak in the FL2 channels presented a better correlation with M_{BC}/PM_{800} than that of the total FL2 particles, suggesting a closer link of this peak to combustion process.

3.3 Classification of fluorescent aerosol particles

3.3.1 Spectral patterns of fluorescent aerosol particles

The complex nature of FAPs in polluted areas challenges the interpretation of ambient measurements. Different fluorophores have their characteristic excitation-emission matrices (EEM) map, which can be useful for discrimination of biological from non-biological FAPs (Pöhlker et al., 2012). Since WIBS only has two excitation and emission wavebands, a high-resolution EEM map cannot be retrieved. But we can still consider the two wavebands as a low resolution EEMs, of which the distribution (i.e., the ratio of the two wavebands) may also contain information about the nature of FAPs. For example, we can assume two kinds of fluorescent compounds I and II have different fluorescent spectra, as shown in Fig. 5a. For each compound, the integrated fluorescence intensity are determined in two wavebands by WIBS (Fig. 5b). For qualitative analysis, a normalized EEM is often used providing the relative wavelength dependence of fluorescent materials. For WIBS, we simply used the ratio of fluorescence intensity from different WIBS channels to represent the wavelength dependence (Fig. 5c).

Atmos. Chem. Phys. Discuss., doi:10.5194/acp-2016-228, 2016
Manuscript under review for journal Atmos. Chem. Phys.
Published: 17 March 2016

Atmospheric Chemistry and Physics Discussions

Figure 6 shows the intensity distributions of aerosols particles in different fluorescence bands/channels. Due to the instrument setting, fluorescence signal intensities beyond 2200 arbitrary units (a.u.) are forced to the range of 2000-2200 arbitrary units, regarding as saturated signal. Hence we only discussed fluorescence signal intensities below 2000 arbitrary units. We first investigated the intensity ratio between channel FL1 and FL2, as shown in Fig. 6a. With increasing fluorescence intensity, the number concentrations sharply dropped, i.e., most of the abundant aerosol particles exhibited no or only weak fluorescence. Using the intensity ratio of FL1 to FL2 (I_{FL1}/I_{FL2}) as a fluorescence fingerprint, we obtained two prominent groups of aerosols with I_{FL1}/I_{FL2} approaching 0 or infinity. $I_{FL1}/I_{FL2} \sim 0$ means that the aerosol have a low FL1 intensity below the detection limit and a high FL2 intensity, while I_{FL1}/I_{FL2} approaching infinity means the opposite. According to the detection thresholds of both FL1 and FL2 channels, we then classified the aerosol particles into four groups with FL1/FL2 above or below the detection threshold (labelled as g1 to g4 in Fig. 6). We further investigated the FL3 properties of the various groups. As shown in Figs. 6b-d, the aerosol number concentration decreased as FL3 intensity increased resembling the distribution for FL1 and FL2. Similarly we used the fluorescence threshold of FL3 to classify aerosols from g1 to g4 into subgroups.

Our efforts towards a spectral fingerprint resulted in the same classification method as in Perring et al. (2015). Here we adopted the labels of Perring et al. (2015) in which channel A refers to FL1, channel B refers to FL2 and channel C refers to FL3. Any aerosol particle can have signals above/below the fluorescence threshold in any of these channels, leading to seven combinations of fluorescence signals, i.e., particles with fluorescence signals above the threshold in single channel as types A, B and C; particles with fluorescence signals in two channels as types AB, AC and BC and particles with fluorescence signals in all three channels as type ABC (Table 1).

As shown in Fig.7a, types B, BC and C were the most abundant FAPs, followed by types ABC, AB and A. Type AC had the lowest loading and was not even visible. The mean number concentrations of dominant types B, BC and C were 1.77 cm^{-3}, 1.06 cm^{-3} and 0.66 cm^{-3}, respectively (Table 4). Meanwhile, the number fractions of types A, AB, and ABC showed good correlations with M_{BC}/PM_{800} (Fig. 8), suggesting a large

Atmos. Chem. Phys. Discuss., doi:10.5194/acp-2016-228, 2016
Manuscript under review for journal Atmos. Chem. Phys.
Published: 17 March 2016

Atmospheric Chemistry and Physics Discussions

contribution of combustion-generated aerosol particles to these types. Note that all these types contain FL1 signals, implying the potential application of FL1 in the identification of biomass burning (or other combustions) events. Likewise, fluorescent types B and BC mostly followed the variation of M_{BC}/PM_{800} except for November 8 when elevated fractional contributions were observed one day before a rain event on November 9. A dramatic release of certain fungal spores was often observed before rain (Hjelmroos, 1993). However, the increase on November 8 was mainly contributed by 1-2 μm FAPs rather than larger than 3 μm fungal spores shown by Hjelmroos (1993). So the origin of this elevated FAPs remained inconclusive. Fluorescent type C showed a weak negative correlation with M_{BC}/PM_{800}, suggesting a minor role of combustion-generated aerosols or major contribution of non-combustion related aerosols (e.g., bioaerosols or dusts).

3.3.2 Fluorescence intensity

Besides the relative wavelength dependence, the absolute quantum yield is also one of the most important characteristics of a fluorophore. Discrepancies in the quantum yield can directly influence the fluorescence, resulting in different intensity levels. Thus it is possible to use the intensity information to identify different kinds of FAPs. Huffman et al. (2012) showed that the UV-APS can be used to successfully discriminate bioaerosols from dust particles, both of which have been suggested to fluoresce (Pöhlker et al., 2012). Since FL3 is running in a similar excitation-emission wavelength as the UV-APS, we suggest that the FL3 channel can be used to discriminate bioaerosols from combustion-generated FAPs in a similar approach.

We first made a hypothesis that there exists a characteristic intensity value I_{cri} (in FL3 channel), above which most FAPs are bioaerosols. Since I_{cri} cannot be directly inferred from the intensity distribution (Fig. 6), we adopted the parameter M_{BC}/PM_{800} to assist our analysis. This is because bioaerosols and combustion-generated FAPs are of different origins, we scanned different values for I_{cri} until the corresponding FAPs (of intensity> I_{cri}) fraction showed a non-positive correlation with M_{BC}/PM_{800}.

Figure 9 shows the averaged fractional contribution of FAPs with $I_{FL3}>I_{cri}$ at different M_{BC}/PM_{800} levels. To account for the size dependence of fluorescence signals, we first classified FAPs according to the particle size. For the 1-2 μm size range, the fraction was always positively correlated with M_{BC}/PM_{800} and was independent of the

Atmos. Chem. Phys. Discuss., doi:10.5194/acp-2016-228, 2016
Manuscript under review for journal Atmos. Chem. Phys.
Published: 17 March 2016

Atmospheric Chemistry and Physics Discussions

selection of I_{cri}. For the size range of 2-5 μm, the FAPs showed mostly negative correlation with M_{BC}/PM_{800} and were also independent of the I_{cri} selection. For FAPs larger than 5 μm, the selection of I_{cri} became critical. With increasing I_{cri}, the dependence of FL3 fraction on M_{BC}/PM_{800} gradually became weaker and finally turned to negative at I_{cri} > 80 arbitrary units. The results at 5-15 μm were consistent with our hypothesis that bioaerosols have stronger fluorescence intensity than combustion-generated aerosol particles and can be discriminated from their fluorescence intensity. The different correlation statistics of 1-2 μm and 2-5 μm may be explained by the different abundance of bioaerosols and combustion-generated aerosols at different size range. The 2-5 μm mode was dominated by bioaerosols, while the 1-2 μm mode was dominated by combustion-generated aerosol particles. Therefore there was no clear dependence on the selection of I_{cri}. Saari et al. (2015) reported that FAPs at 0.5-1.5 μm might be due to anthropogenic emissions such as biomass burning, while most fungal spores and pollen dominated the larger size range (Després et al., 2012). It is also possible that I_{cri} had a size dependence because different types of bioaerosols may dominate different size ranges.

By integrating the FAPs of different correlations with M_{BC}/PM_{800}, we retrieved the number concentrations of "non-combustion-related" (NCR) type particles (FAPs with I_{FL3}>18 arbitrary units at 2-5 μm and FAPs with I_{FL3}>80 arbitrary units at 5-15 μm) and "combustion-related" (CR) type particles (FAPs with I_{FL3}>18 arbitrary units at 1-2 μm and FAPs with $I_{FL3}\leq$80 at 5-15 μm). The mean number concentrations of NCR type and CR type particles were 0.59±0.42 cm^{-3} and 1.50±1.09 cm^{-3}, respectively. The NCR type FAPs are likely bioaerosols.

In this study, we applied two methods to classify FAPs measured by WIBS, resulting in two non-combustion-types of particles: type C particles derived from fluorescent spectral pattern analysis and NCR type particles derived from fluorescence intensity pattern analysis. As shown in Fig. 10, the mean number concentrations of type C and NCR type particle were 0.66 cm^{-3} and 0.59 cm^{-3}, which were still higher than those found in PBAPs-dominated regions like the Amazon (Huffman et al., 2012), Hyytiälä (Schumacher et al., 2013) and PdD (Gabey et al., 2013). This indicates that still a residual

Atmos. Chem. Phys. Discuss., doi:10.5194/acp-2016-228, 2016
Manuscript under review for journal Atmos. Chem. Phys.
Published: 17 March 2016

of these non-combustion type particles may comprise other fluorescent constituents like mineral dusts (Miyakawa et al., 2015; Perring et al., 2015).

4. Summary

On-line measurements of FAPs have been performed in Nanjing by using WIBS in the autumn of 2013. Our results showed that the number concentrations of FAPs were 1~2 order of magnitudes higher than those reported in previous studies. The observed high values suggested that directly using FL1, FL2 and FL3 channels to index PBAPs is not suitable for polluted areas. The number fraction of FL1 showed strong correlation with M_{BC}/PM_{800} (r=0.748), indicative of a strong bias by anthropogenic emissions.

In this study, we used two methods to classify the FAPs. According to the threshold of each channel, FAPs were divided into 7 types. Number fraction of type C showed negative correlation (r=-0.125) with M_{BC}/PM_{800}, which might be more representative for bioaerosols. Meanwhile, on the basis of the FL3 fluorescent intensity and its correlations with M_{BC}/PM_{800}, FL3 fluorescent particles were divided into 2 types. Combustion-generated type particles seemed to dominate 1-2 μm, while the non-combustion-related type particles, which concentrated in the size range of 2-5 μm and showed negative correlation (r=-0.211) with M_{BC}/PM_{800}, might be originated from biological emissions. The number concentrations of the identified two types of bioaerosols (0.66 cm^{-3} for type C particles and 0.59 cm^{-3} for non-combustion-related type), however, were still higher than those observed in clean background areas, indicating they may also include some other fluorophores, such as dusts.

Our results suggested that fluorescence measurements in polluted areas are prone to interferences and uncertainty introduced by the anthropogenic emissions. Discrimination of biological particles from FAPs still needs further development. Each fluorophore species presents unique fluorescence spectrum, hence we can effectively distinguish biological particles from other FAPs based on their specific EEM maps. Due to the limitation of excitation and emission wavebands of WIBS, the development of a multi-wavebands instrument is hence needed. Other methods such as the cluster analysis (Robinson et al., 2013; Crawford et al., 2014; Crawford et al., 2015) also exhibited the ability to differentiate various FAPs. Measuring additional particle properties such as size

Atmos. Chem. Phys. Discuss., doi:10.5194/acp-2016-228, 2016
Manuscript under review for journal Atmos. Chem. Phys.
Published: 17 March 2016

Atmospheric Chemistry and Physics Discussions

335 and morphology will help ameliorate the interferences by providing additional
336 dimensions to distinguish fluorescent particles of different emission mechanisms.
337

Atmos. Chem. Phys. Discuss., doi:10.5194/acp-2016-228, 2016
Manuscript under review for journal Atmos. Chem. Phys.
Published: 17 March 2016

Atmospheric Chemistry and Physics Discussions

Acknowledgments

This study was supported by the Max Plank Society (MPG), the European Commission under the projects BACCHUS (Grant No. 603445) and the Natural Science Foundation of China (Project No. 91544103). Xiawei Yu and Minghui Zhang would like to thank the China Scholarship Council (CSC) for financial support. We thank the SORPES-NJU station for logistic and instrumentation support.

Atmos. Chem. Phys. Discuss., doi:10.5194/acp-2016-228, 2016
Manuscript under review for journal Atmos. Chem. Phys.
Published: 17 March 2016

Atmospheric Chemistry and Physics Discussions

References

Bary, A., Garnsey, H. E. F., and Balfour, I. B.: Comparative morphology and biology of the fungi, mycetozoa and bacteria, Clarendon Press, 1887.

Brosseau, L. M., Vesley, D., Rice, N., Goodell, K., Nellis, M., and Hairston, P.: Differences in Detected Fluorescence Among Several Bacterial Species Measured with a Direct-Reading Particle Sizer and Fluorescence Detector, Aerosol Sci. Technol., 32, 545-558, 10.1080/027868200303461, 2000.

Cao, C., Jiang, W., Wang, B., Fang, J., Lang, J., Tian, G., Jiang, J., and Zhu, T. F.: Inhalable Microorganisms in Beijing's PM2.5 and PM10 Pollutants during a Severe Smog Event, Environ Sci Technol, 48, 1499-1507, 10.1021/es4048472, 2014.

Chang, J. L., and Thompson, J. E.: Characterization of colored products formed during irradiation of aqueous solutions containing H 2 O 2 and phenolic compounds, Atmos. Environ., 44, 541-551, 2010.

Christner, B. C., Morris, C. E., Foreman, C. M., Cai, R., and Sands, D. C.: Ubiquity of Biological Ice Nucleators in Snowfall, Science, 319, 1214, 10.1126/science.1149757, 2008.

Crawford, I., Robinson, N. H., Flynn, M. J., Foot, V. E., Gallagher, M. W., Huffman, J. A., Stanley, W. R., and Kaye, P. H.: Characterisation of bioaerosol emissions from a Colorado pine forest: results from the BEACHON-RoMBAS experiment, Atmos Chem Phys, 14, 8559-8578, 10.5194/acp-14-8559-2014, 2014.

Crawford, I., Ruske, S., Topping, D. O., and Gallagher, M. W.: Evaluation of hierarchical agglomerative cluster analysis methods for discrimination of primary biological aerosol, Atmos. Meas. Tech., 8, 4979-4991, 10.5194/amt-8-4979-2015, 2015.

Creamean, J. M., Suski, K. J., Rosenfeld, D., Cazorla, A., DeMott, P. J., Sullivan, R. C., White, A. B., Ralph, F. M., Minnis, P., Comstock, J. M., Tomlinson, J. M., and Prather, K. A.: Dust and Biological Aerosols from the Sahara and Asia Influence Precipitation in the Western U.S, Science, 339, 1572-1578, 10.1126/science.1227279, 2013.

DeLeon-Rodriguez, N., Lathem, T. L., Rodriguez-R, L. M., Barazesh, J. M., Anderson, B. E., Beyersdorf, A. J., Ziemba, L. D., Bergin, M., Nenes, A., and Konstantinidis, K. T.: Microbiome of the upper troposphere: Species composition and prevalence, effects of tropical storms, and atmospheric implications, P Natl Acad Sci USA, 10.1073/pnas.1212089110, 2013.

Després, V. R., Huffman, J. A., Burrows, S. M., Hoose, C., Safatov, A. S., Buryak, G., Fröhlich-Nowoisky, J., Elbert, W., Andreae, M. O., Pöschl, U., and Jaenicke, R.: Primary biological aerosol particles in the atmosphere: a review, Tellus B, 64, 2012.

Ding, A. J., Fu, C. B., Yang, X. Q., Sun, J. N., Zheng, L. F., Xie, Y. N., Herrmann, E., Nie, W., Petäjä, T., Kerminen, V. M., and Kulmala, M.: Ozone and fine particle in the western Yangtze River Delta: an overview of 1 yr data at the SORPES station, Atmos Chem Phys, 13, 5813-5830, 10.5194/acp-13-5813-2013, 2013.

Duchaine, C., Thorne, P. S., Mériaux, A., Grimard, Y., Whitten, P., and Cormier, Y.: Comparison of endotoxin exposure assessment by bioaerosol impinger and filter-sampling methods, Appl. Environ. Microbiol., 67, 2775-2780, 2001.

Gabey, A. M., Gallagher, M. W., Whitehead, J., Dorsey, J. R., Kaye, P. H., and Stanley, W. R.: Measurements and comparison of primary biological aerosol above and below a tropical forest canopy using a dual channel fluorescence spectrometer, Atmos Chem Phys, 10, 4453-4466, 10.5194/acp-10-4453-2010, 2010.

Gabey, A. M., Stanley, W. R., Gallagher, M. W., and Kaye, P. H.: The fluorescence properties of aerosol larger than 0.8 μm in urban and tropical rainforest locations, Atmos Chem Phys, 11, 5491-5504, 10.5194/acp-11-5491-2011, 2011.

Gabey, A. M., Vaitilingom, M., Freney, E., Boulon, J., Sellegri, K., Gallagher, M. W., Crawford, I. P., Robinson, N. H., Stanley, W. R., and Kaye, P. H.: Observations of fluorescent and

396 biological aerosol at a high-altitude site in central France, Atmos Chem Phys, 13, 7415-7428,
397 10.5194/acp-13-7415-2013, 2013.
398 Griffin, D. W.: Atmospheric movement of microorganisms in clouds of desert dust and
399 implications for human health, Clin. Microbiol. Rev., 20, 459-477, Doi 10.1128/Cmr.00039-06,
400 2007.
401 Hairston, P. P., Ho, J., and Quant, F. R.: Design of an instrument for real-time detection of
402 bioaerosols using simultaneous measurement of particle aerodynamic size and intrinsic
403 fluorescence, J. Aerosol Sci., 28, 471-482, Doi 10.1016/S0021-8502(96)00448-X, 1997.
404 Haldane, J., and Anderson, A.: The carbonic acid, organic matter, and micro-organisms in air,
405 more especially of dwellings and schools, Philosophical Transactions of the Royal Society of
406 London. B, 61-111, 1887.
407 Hallar, A. G., Chirokova, G., McCubbin, I., Painter, T. H., Wiedinmyer, C., and Dodson, C.:
408 Atmospheric bioaerosols transported via dust storms in the western United States, Geophys. Res.
409 Lett., 38, L17801, 10.1029/2011GL048166, 2011.
410 Healy, D. A., O'Connor, D. J., Burke, A. M., and Sodeau, J. R.: A laboratory assessment of the
411 Waveband Integrated Bioaerosol Sensor (WIBS-4) using individual samples of pollen and fungal
412 spore material, Atmos. Environ., 60, 534-543, http://dx.doi.org/10.1016/j.atmosenv.2012.06.052,
413 2012.
414 Healy, D. A., Huffman, J. A., O'Connor, D. J., Pöhlker, C., Pöschl, U., and Sodeau, J. R.:
415 Ambient measurements of biological aerosol particles near Killarney, Ireland: a comparison
416 between real-time fluorescence and microscopy techniques, Atmos Chem Phys, 14, 8055-8069,
417 10.5194/acp-14-8055-2014, 2014.
418 Henningson, E. W., and Ahlberg, M. S.: Evaluation of microbiological aerosol samplers: a review,
419 J. Aerosol Sci., 25, 1459-1492, 1994.
420 Herrmann, E., Ding, A. J., Kerminen, V. M., Petäjä, T., Yang, X. Q., Sun, J. N., Qi, X. M.,
421 Manninen, H., Hakala, J., Nieminen, T., Aalto, P. P., Kulmala, M., and Fu, C. B.: Aerosols and
422 nucleation in eastern China: first insights from the new SORPES-NJU station, Atmos Chem Phys,
423 14, 2169-2183, 10.5194/acp-14-2169-2014, 2014.
424 Hjelmroos, M.: Relationship between airborne fungal spore presence and weather variables:
425 Cladosporium and Alternaria, Grana, 32, 40-47, 1993.
426 Huffman, J. A., Treutlein, B., and Pöschl, U.: Fluorescent biological aerosol particle
427 concentrations and size distributions measured with an Ultraviolet Aerodynamic Particle Sizer
428 (UV-APS) in Central Europe, Atmos Chem Phys, 10, 3215-3233, 10.5194/acp-10-3215-2010,
429 2010.
430 Huffman, J. A., Sinha, B., Garland, R. M., Snee-Pollmann, A., Gunthe, S. S., Artaxo, P., Martin,
431 S. T., Andreae, M. O., and Pöschl, U.: Size distributions and temporal variations of biological
432 aerosol particles in the Amazon rainforest characterized by microscopy and real-time UV-APS
433 fluorescence techniques during AMAZE-08, Atmos Chem Phys, 12, 11997-12019, 10.5194/acp-
434 12-11997-2012, 2012.
435 Huffman, J. A., Prenni, A. J., DeMott, P. J., Pöhlker, C., Mason, R. H., Robinson, N. H.,
436 Fröhlich-Nowoisky, J., Tobo, Y., Després, V. R., Garcia, E., Gochis, D. J., Harris, E., Müller-
437 Germann, I., Ruzene, C., Schmer, B., Sinha, B., Day, D. A., Andreae, M. O., Jimenez, J. L.,
438 Gallagher, M., Kreidenweis, S. M., Bertram, A. K., and Pöschl, U.: High concentrations of
439 biological aerosol particles and ice nuclei during and after rain, Atmos Chem Phys, 13, 6151-
440 6164, 10.5194/acp-13-6151-2013, 2013.
441 Miyakawa, T., Kanaya, Y., Taketani, F., Tabaru, M., Sugimoto, N., Ozawa, Y., and Takegawa, N.:
442 Ground-based measurement of fluorescent aerosol particles in Tokyo in the spring of 2013:
443 Potential impacts of nonbiological materials on autofluorescence measurements of airborne
444 particles, J Geophys Res-Atmos, 2014JD022189, 10.1002/2014JD022189, 2015.
445 Morris, C. E., Sands, D. C., Glaux, C., Samsatly, J., Asaad, S., Moukahel, A. R., Gonçalves, F. L.
446 T., and Bigg, E. K.: Urediospores of rust fungi are ice nucleation active at > −10 °C and harbor

447 ice nucleation active bacteria, Atmos Chem Phys, 13, 4223-4233, 10.5194/acp-13-4223-2013,
448 2013.
449 Perring, A. E., Schwarz, J. P., Baumgardner, D., Hernandez, M. T., Spracklen, D. V., Heald, C. L.,
450 Gao, R. S., Kok, G., McMeeking, G. R., McQuaid, J. B., and Fahey, D. W.: Airborne
451 observations of regional variation in fluorescent aerosol across the United States, J Geophys Res-
452 Atmos, 120, 1153-1170, 10.1002/2014JD022495, 2015.
453 Pöhlker, C., Huffman, J. A., and Pöschl, U.: Autofluorescence of atmospheric bioaerosols –
454 fluorescent biomolecules and potential interferences, Atmos. Meas. Tech., 5, 37-71, 10.5194/amt-
455 5-37-2012, 2012.
456 Polymenakou, P. N., Mandalakis, M., Stephanou, E. G., and Tselepides, A.: Particle size
457 distribution of airborne microorganisms and pathogens during an intense African dust event in the
458 eastern Mediterranean, Environ. Health Perspect., 116, 292-296, Doi 10.1289/Ehp.10684, 2008.
459 Pöschl, U.: Atmospheric aerosols: Composition, transformation, climate and health effects,
460 Angewandte Chemie-International Edition, 44, 7520-7540, DOI 10.1002/anie.200501122, 2005.
461 Pöschl, U., Martin, S. T., Sinha, B., Chen, Q., Gunthe, S. S., Huffman, J. A., Borrmann, S.,
462 Farmer, D. K., Garland, R. M., Helas, G., Jimenez, J. L., King, S. M., Manzi, A., Mikhailov, E.,
463 Pauliquevis, T., Petters, M. D., Prenni, A. J., Roldin, P., Rose, D., Schneider, J., Su, H., Zorn, S.
464 R., Artaxo, P., and Andreae, M. O.: Rainforest Aerosols as Biogenic Nuclei of Clouds and
465 Precipitation in the Amazon, Science, 329, 1513-1516, 10.1126/science.1191056, 2010.
466 Robinson, N. H., Allan, J. D., Huffman, J. A., Kaye, P. H., Foot, V. E., and Gallagher, M.:
467 Cluster analysis of WIBS single-particle bioaerosol data, Atmos. Meas. Tech., 6, 337-347,
468 10.5194/amt-6-337-2013, 2013.
469 Saari, S., Niemi, J., Rönkkö, T., Kuuluvainen, H., Järvinen, A., Pirjola, L., Aurela, M., Hillamo,
470 R., and Keskinen, J.: Seasonal and Diurnal Variations of Fluorescent Bioaerosol Concentration
471 and Size Distribution in the Urban Environment, Aerosol and Air Quality Research, 15, 572-581,
472 2015.
473 Schumacher, C. J., Pöhlker, C., Aalto, P., Hiltunen, V., Petäjä, T., Kulmala, M., Pöschl, U., and
474 Huffman, J. A.: Seasonal cycles of fluorescent biological aerosol particles in boreal and semi-arid
475 forests of Finland and Colorado, Atmos Chem Phys, 13, 11987-12001, 10.5194/acp-13-11987-
476 2013, 2013.
477 Toprak, E., and Schnaiter, M.: Fluorescent biological aerosol particles measured with the
478 Waveband Integrated Bioaerosol Sensor WIBS-4: laboratory tests combined with a one year field
479 study, Atmos Chem Phys, 13, 225-243, 10.5194/acp-13-225-2013, 2013.
480 Wang, H., Zhu, B., Shen, L., Liu, X., Zhang, Z., and Yang, Y.: Size distributions of aerosol
481 during the Spring Festival in Nanjing, Huan jing ke xue (in Chinese), 35, 442-450, 2014.
482 Wei, K., Zou, Z., Zheng, Y., Li, J., Shen, F., Wu, C.-y., Wu, Y., Hu, M., and Yao, M.: Ambient
483 bioaerosol particle dynamics observed during haze and sunny days in Beijing, Sci. Total Environ.,
484 550, 751-759, http://dx.doi.org/10.1016/j.scitotenv.2016.01.137, 2016.
485 Yu, J., Hu, Q., Xie, Z., Kang, H., Li, M., Li, Z., and Ye, P.: Concentration and Size Distribution
486 of Fungi Aerosol over Oceans along a Cruise Path during the Fourth Chinese Arctic Research
487 Expedition, Atmosphere, 4, 337-348, 2013.

488

489

Atmos. Chem. Phys. Discuss., doi:10.5194/acp-2016-228, 2016
Manuscript under review for journal Atmos. Chem. Phys.
Published: 17 March 2016

Atmospheric Chemistry and Physics Discussions

490 # Tables

491 **Table 1.** Definition of abbreviations used in the text.

Short name	Description
PBAPs	Primary biological aerosol particles
FAPs	Fluorescent aerosol particles
FL1	Fluorescent detected in channel F1 280 (excitation at 280 nm, detection 310–400 nm)
FL2	Fluorescent detected in channel F2 280 (excitation at 280 nm, detection 420–650 nm)
FL3	Fluorescent detected in channel F2 370 (excitation at 370 nm, detection 420–650 nm)
N_T	Number of all particles measured by WIBS-4
N_{FL1}	Number of fluorescent particles in channel FL1
N_{FL2}	Number of fluorescent particles in channel FL2
N_{FL3}	Number of fluorescent particles in channel FL3
F_{FL1}	Fraction of particles in channel FL1
F_{FL2}	Fraction of particles in channel FL2
F_{FL3}	Fraction of particles in channel FL3
M_{BC}	Mass concentration of black carbon
PM_{800}	Mass concentration of particles in the size range of 6-800 nm
D_o	Particle optical equivalent diameter
a.u.	Arbitrary units
Type A	Fluorescent particle signal in channel FL1 only
Type B	Fluorescent particle signal in channel FL2 only
Type C	Fluorescent particle signal in channel FL3 only
Type AB	Fluorescent particle signal in channels FL1 and FL2
Type AC	Fluorescent particle signal in channels FL1 and FL3
Type BC	Fluorescent particle signal in channels FL2 and FL3
Type ABC	Fluorescent particle signal in channels FL1, FL2 and FL3

492

493

Atmos. Chem. Phys. Discuss., doi:10.5194/acp-2016-228, 2016
Manuscript under review for journal Atmos. Chem. Phys.
Published: 17 March 2016

Atmospheric Chemistry and Physics Discussions

494 **Table 2.** Integrated number concentrations of total and fluorescent particles. *N* is number
495 concentration (cm^{-3}), *F* is the ratio of fluorescent particles to total particles.

	N_T	N_{FL1}	N_{FL2}	N_{FL3}	F_{FL1} (%)	F_{FL2} (%)	F_{FL3} (%)
10th percentile	5.45	0.19	1.11	0.66	2.21	17.25	10.08
Mean	13.09	0.57	3.35	2.09	4.59	25.32	15.59
Median	10.74	0.44	2.77	1.67	4.27	25.57	15.63
90th percentile	23.83	1.16	6.52	4.20	7.57	32.38	20.68
Standard deviation	8.84	0.46	2.33	1.45	2.23	5.99	3.90

496
497

Atmos. Chem. Phys. Discuss., doi:10.5194/acp-2016-228, 2016
Manuscript under review for journal Atmos. Chem. Phys.
Published: 17 March 2016

Atmospheric Chemistry and Physics Discussions

498 **Table 3.** The comparisons between the results of this study and previous studies. Unit of
499 fluorescent particles is L^{-1}. Numbers in brackets are the number fractions of fluorescent
500 particles.

Site Location	Site Category	Season	FL1	FL2	FL3	FAPs	References
Nanjing,China	sub-urban	autumn	570 (4.6%)	3350 (25.3%)	2090 (15.6%)	-	This study
Manchester, UK	urban	winter	29 (2.1%)	52 (3.7%)	110 (7.8%)	-	(Gabey et al., 2011)
Puy de Dôme mountain, France	high-altitude	summer	12	-	94	-	(Gabey et al., 2013)
Killarney, Ireland	rural	summer	175 (0.5%)	95 (0.3%)	35 (0.1%)	15 (0.05%)[a]	(Healy et al., 2014)
Borneo, Malaysis	rainforest	summer	-	-	-	150 [b]	(Gabey et al., 2010)
Karlsruhe, Germany	semi-rural	spring,summer, autumn, winter	-	-	-	30 (5.3%) [b]	(Toprak and Schnaiter, 2013)
Amazon, Brazil	rainforest	spring	-	-	-	93 (24%) [a]	(Huffman et al., 2012)
Mainz, Germany	semi-urban	summer, autumn, winter	-	-	-	27 (4%) [a]	(Huffman et al., 2010)
Helsinki, Finland	urban	summer	-	-	-	13 (8%) [a]	(Saari et al., 2015)
Hyytiälä, Finland	boreal forest	spring	-	-	-	15 (4.4%) [a]	(Schumacher et al., 2013)
		summer	-	-	-	46 (13%) [a]	
		autumn	-	-	-	27 (9.8%) [a]	
		winter	-	-	-	4 (1.1%) [a]	
Colorado, USA	rural	spring	-	-	-	15 (2.5%) [a]	(Schumacher et al., 2013)
		summer	-	-	-	30 (8.8%) [a]	
		autumn	-	-	-	17 (5.7%) [a]	
		winter	-	-	-	5.3 (0.3%) [a]	

501 a: results of UV-APS

502 b: combine with FL1 and FL3 channel

503

Atmos. Chem. Phys. Discuss., doi:10.5194/acp-2016-228, 2016
Manuscript under review for journal Atmos. Chem. Phys.
Published: 17 March 2016

Atmospheric Chemistry and Physics Discussions

504 **Table 4.** Integrated mean number concentrations of each type particles. *N* is number
505 concentration (cm^{-3}), fraction is the ratio of each type particles to total particles.

	NCR type	CR type	type A	type B	type C	type AB	type AC	type ABC	type BC
N (cm^{-3})	0.59	1.50	0.05	1.77	0.66	0.15	0.003	0.37	1.06
Fraction (%)	4.69	10.91	0.45	12.95	4.40	1.20	0.03	2.91	8.26

506

Atmos. Chem. Phys. Discuss., doi:10.5194/acp-2016-228, 2016
Manuscript under review for journal Atmos. Chem. Phys.
Published: 17 March 2016

Atmospheric Chemistry and Physics Discussions

507 # Figures

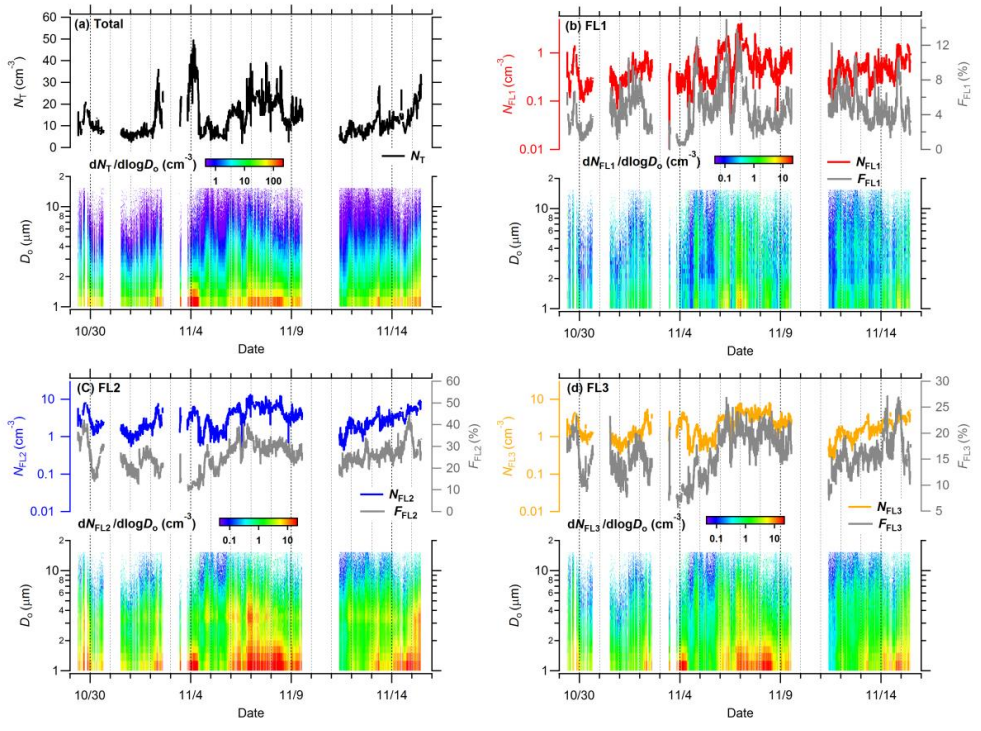

508

509 **Figure 1.** Time series of number concentrations and number size distributions of (a) total
510 aerosol particles and fluorescent aerosol particles in channel (b) FL1, (c) FL2, and (d)
511 FL3. In panel top halves, N_T, N_{FL1}, N_{FL2}, and N_{FL3} represent the number concentrations of
512 total aerosol particles and fluorescent aerosol particles in different channels. F_{FL1}, F_{FL2},
513 and F_{FL3} represent the number fractions of fluorescent aerosol particles in total aerosol
514 particles. The panel bottom halves show the number size distributions of total and
515 fluorescent aerosol particles.

516

Atmos. Chem. Phys. Discuss., doi:10.5194/acp-2016-228, 2016
Manuscript under review for journal Atmos. Chem. Phys.
Published: 17 March 2016

Atmospheric Chemistry and Physics Discussions

517

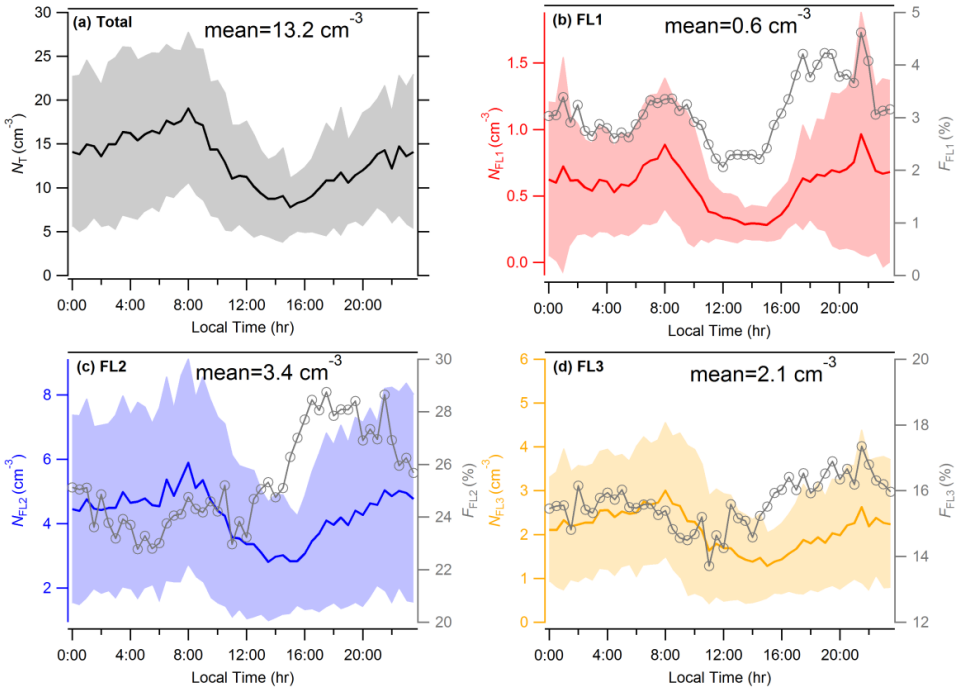

518
519 **Figure 2.** Diurnal variations of number concentrations of (a) total aerosol particles and
520 fluorescent aerosol particles in channel (b) FL1, (c) FL2, and (d) FL3. Gray line indicates
521 the number fraction of respective fluorescent particles (right axis). Shading indicates ±
522 one standard deviation.

523

524

Atmos. Chem. Phys. Discuss., doi:10.5194/acp-2016-228, 2016
Manuscript under review for journal Atmos. Chem. Phys.
Published: 17 March 2016

Atmospheric Chemistry and Physics Discussions

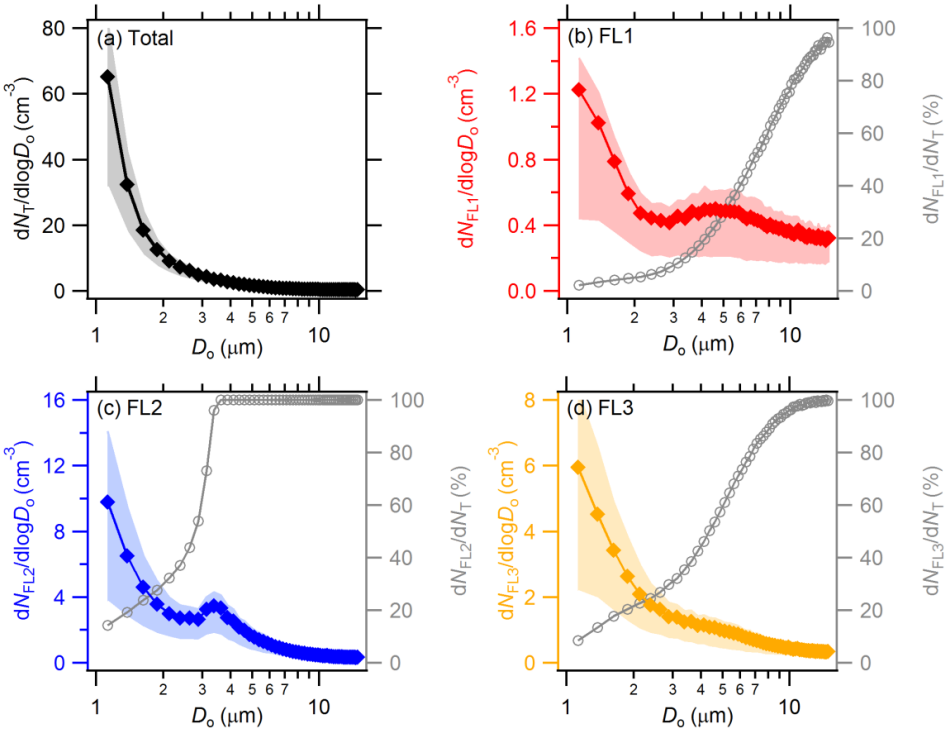

525

526 **Figure 3.** Mean (solid diamond) number size distributions of (a) Total particles, black
527 and fluorescent aerosol particles in channel (b) FL1, red, (c) FL2, blue and (d) FL3,
528 yellow. Open cycles represent the mean fraction of fluorescent aerosol particles to total
529 aerosol particles (right axis) and shaded zones indicate 25th and 75th percentiles.

530

531

Atmos. Chem. Phys. Discuss., doi:10.5194/acp-2016-228, 2016
Manuscript under review for journal Atmos. Chem. Phys.
Published: 17 March 2016

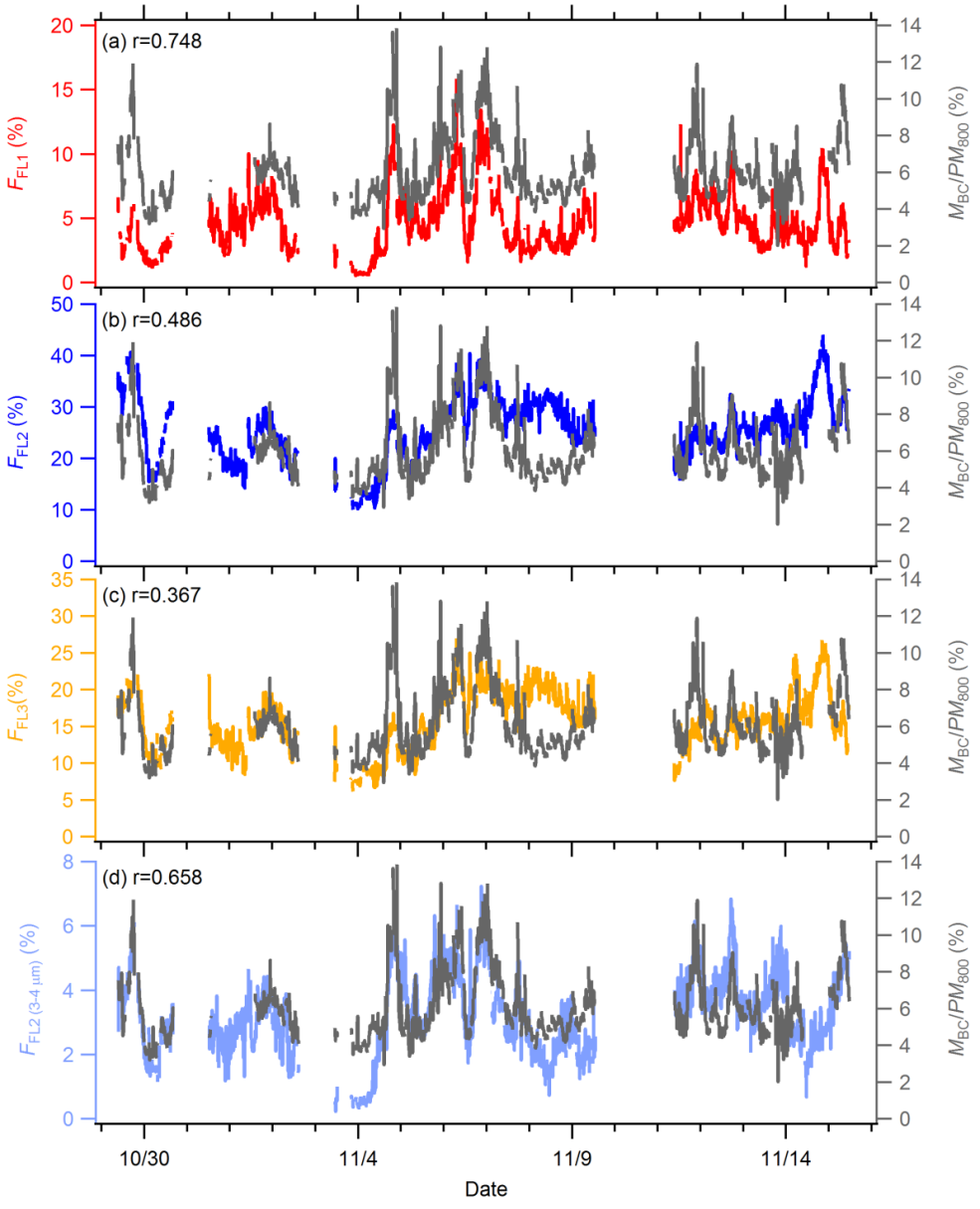

Figure 4. Time series of M_{BC}/PM_{800} (gray line, right axis) and relative number fractions of fluorescent particles in each channel (left axis). (a) F_{FL1}, red line. (b) F_{FL2}, blue line. (c) F_{FL3}, yellow line. (d) F_{FL2} (3-4 μm), light blue: number fraction of FL2 in the size range of 3-4 μm.

Atmos. Chem. Phys. Discuss., doi:10.5194/acp-2016-228, 2016
Manuscript under review for journal Atmos. Chem. Phys.
Published: 17 March 2016

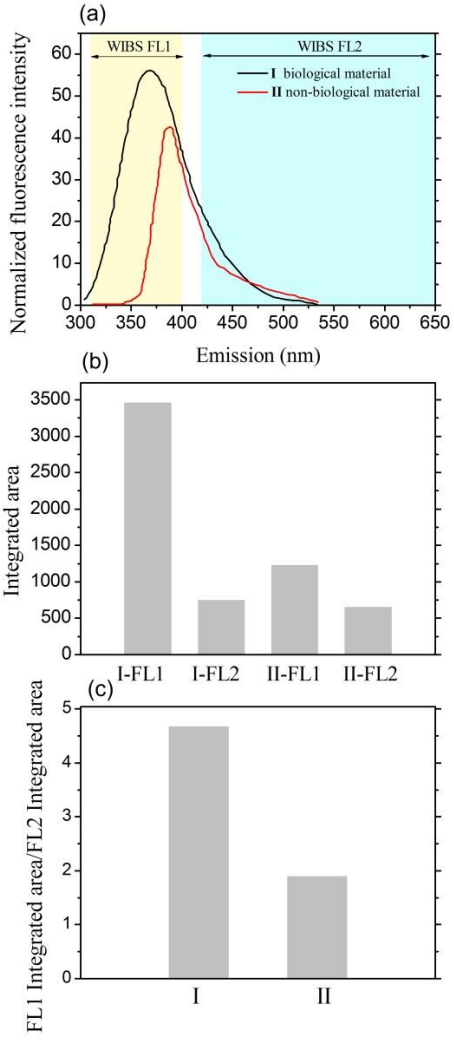

Figure 5. (a) Normalized fluorescence emission spectra of two fluorescent compounds: I (black line, biological material) and II (red line, non-biological material) for excitation wavelengths at λ_{ex}=280 nm. Shadow areas indicate the excitation wavebands of FL1 and FL2 channels of WIBS. (b) Integrated fluorescence intensity of two compounds in two bands (FL1 and FL2). (c) The ratio of fluorescence intensity from different WIBS channels (I_{FL1}/I_{FL2}) of I and II compounds. The fluorescence emission spectra are obtained from Pöhlker et al. (2012).

Atmos. Chem. Phys. Discuss., doi:10.5194/acp-2016-228, 2016
Manuscript under review for journal Atmos. Chem. Phys.
Published: 17 March 2016

Atmospheric Chemistry and Physics Discussions

548

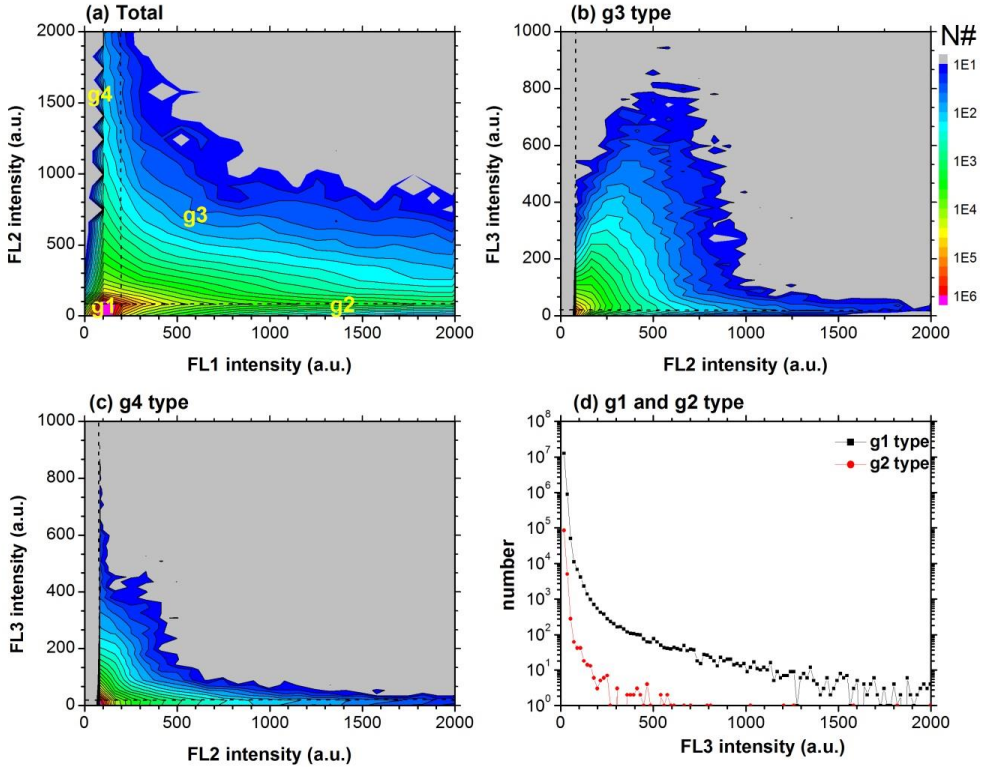

549

550

551 **Figure 6.** Spectral pattern of the classified fluorescence intensity. FL1 intensity is
552 grouped at 100 intervals, FL2 intensity is grouped at 80 intervals and FL3 intensity is
553 grouped at 18 intervals. Color scale is measured particle number. None fluorescent and
554 saturating (FL⩾2000 arbitrary units) aerosol particles were excluded. (a) FL1 intensity
555 versus FL2 intensity of total measured particles; (b) FL2 intensity versus FL3 intensity of
556 g3 type particles; (c) FL2 intensity versus FL3 intensity of g4 type particles; (d) Numbers
557 of g1 and g2 type particles of FL3 fluorescence intensity. Because FL2 intensity of g1
558 and g2 are below the threshold, the spectral patterns are hence not used. Dotted lines
559 denote the threshold of each channel (200 arbitrary units for FL1, 80 arbitrary units for
560 FL2 and 18 arbitrary units for FL3).

561

562

Atmos. Chem. Phys. Discuss., doi:10.5194/acp-2016-228, 2016
Manuscript under review for journal Atmos. Chem. Phys.
Published: 17 March 2016

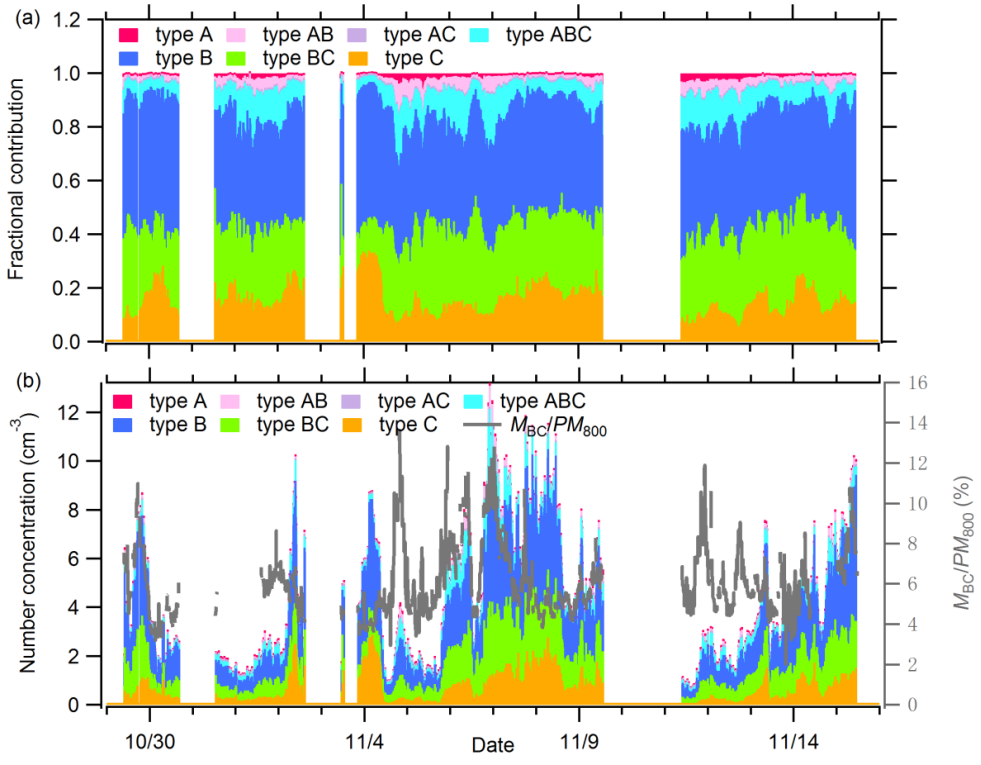

Figure 7. Time series of (a) the fractional contributions of each fluorescent type to the total FAPs and (b) number concentration (left axis) of each fluorescent type and M_{BC}/PM_{800} (gray line, right axis).

Atmos. Chem. Phys. Discuss., doi:10.5194/acp-2016-228, 2016
Manuscript under review for journal Atmos. Chem. Phys.
Published: 17 March 2016

Atmospheric Chemistry and Physics Discussions

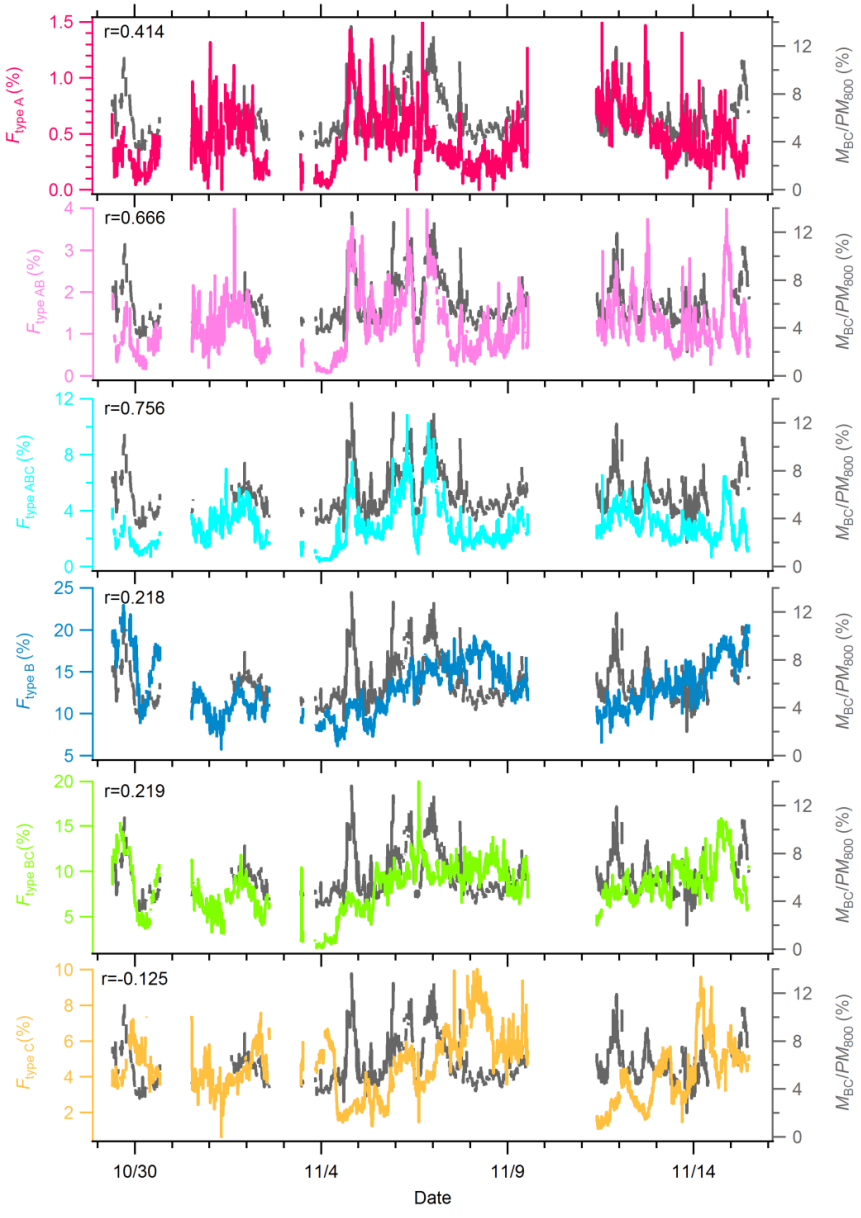

572

573 **Figure 8.** Time series of number fractions of various fluorescent particles (left axis) and

574 M_{BC}/PM_{800} (gray line, right axis).

575

576

Atmos. Chem. Phys. Discuss., doi:10.5194/acp-2016-228, 2016
Manuscript under review for journal Atmos. Chem. Phys.
Published: 17 March 2016

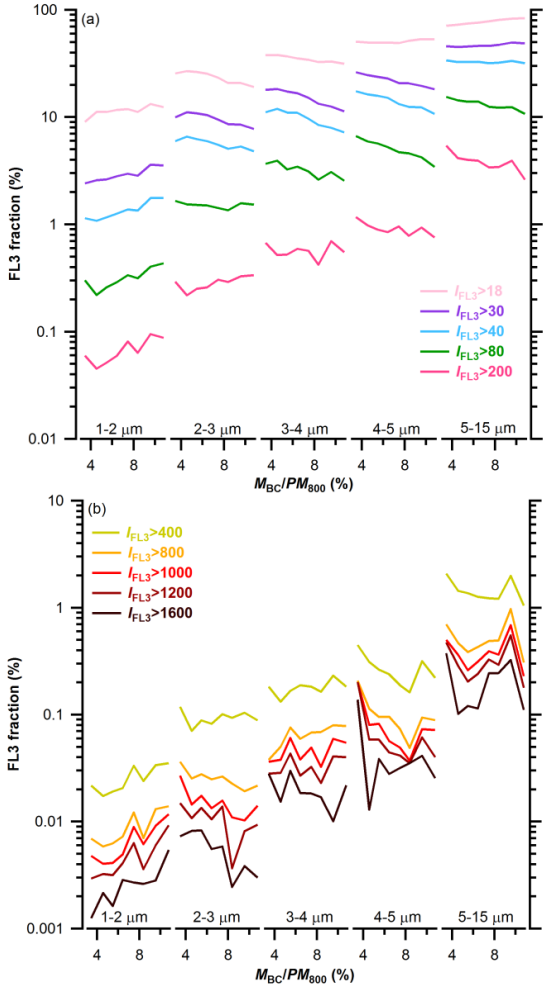

577

578 **Figure 9.** Correlations of FL3 fractions with M_{BC}/PM_{800} in different size ranges. FL3
579 fraction is the number concentration of the subgroup ratio to the number concentration of
580 total particles in each size bin. (a) Low fluorescent intensity group. (b) High fluorescent
581 intensity group. The color lines represent the FL3 intensity (I_{FL3}) above the certain I_{cri}.

582

Atmos. Chem. Phys. Discuss., doi:10.5194/acp-2016-228, 2016
Manuscript under review for journal Atmos. Chem. Phys.
Published: 17 March 2016

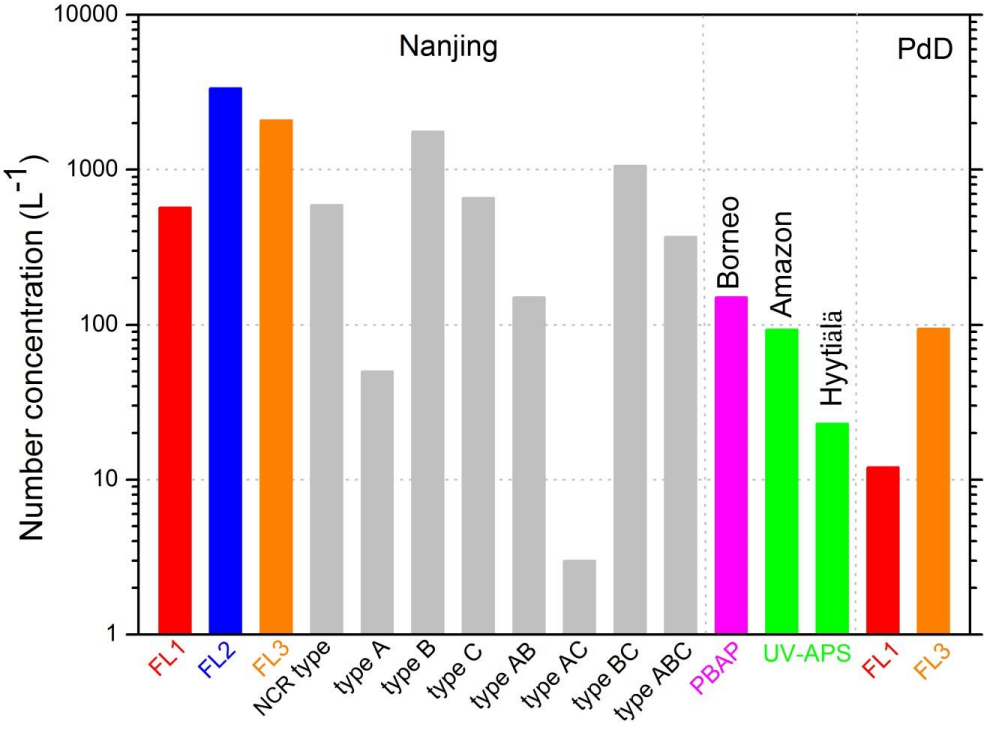

583

584 **Figure 10.** Comparisons of Nanjing data with other previous studies: Puy de Dôme
585 (PdD), France (Gabey et al., 2013); Borneo, Malaysia (Gabey et al., 2010); Amazon
586 (Huffman et al., 2012); Hyytiälä and Colorado(Schumacher et al., 2013). Gray color
587 indicates different type particles of Nanjing.